

A Morphological Study of Alumina Hollow Fiber Membrane

Asrar Al-Obaidy

Chemical Engineering Department, College of Engineering, University of Baghdad
Email: asrarabdullah62@yahoo.com

Abstract

Morphologies of ceramic hollow fiber membranes prepared by a combined phase-inversion and sintering method were studied. The organic binder spinning solution containing suspended Al_2O_3 powders was spun to a hollow fiber precursor, which was then sintered at elevated temperatures (300 °C, 1400 °C, 25 °C) in order to obtain the Al_2O_3 hollow fiber membranes. The spinning solution consisted of polyether sulfone (PES), N-methyl-2-pyrrolidone (NMP), which were used as polymer binder, solvent, respectively. The prepared Al_2O_3 hollow fiber membranes were characterized by a scanning electron microscope (SEM). It is believed that finger-like void formation in asymmetric ceramic membranes is initiated by hydrodynamically unstable viscous fingering developed when a less viscous fluid (non-solvent) is in contact with a higher viscosity fluid (ceramic suspension containing invertible polymer binder). The effects of the air-gap (0 cm, 2 cm, 15 cm) on fibre morphology have been studied and it has been determined that viscosity due to change in air-gap is the dominating factor for ceramic systems.

Keywords: Ceramic membrane, Hollow fiber, Morphology, Phase inversion.

Introduction

Ceramic membranes are convincing particularly in terms of high mechanical, chemical and thermal stability compared to polymeric membranes enabling their use under harsh conditions as well as the application of chemicals and steam for membrane and module/plant cleaning. Therefore, their use in a wide range of different applications from waste water treatment till clarification and sterilization of beverages are well known. Due to their (in principle) unrestricted resistance against organic solvents, ceramic membranes are of particular

interest for organic solvent nano filtration (OSN). This growing new technology describes the application of nano filtration (NF) in pure organic solvents or organic solvent mixtures. OSN has just established during the last 15 years as a result of the development of solvent stable polymeric membranes and offers a high potential for applications in pharmaceutical and chemical industries [1-3].

Many different methods used for preparing inorganic hollow fibers, including dry spinning a system of inorganic material and binder [4], wet spinning a suitable inorganic material-

containing solution and/or solvents [5-9], depositing fibers from the gas phase on to a substrate, or pyrolyzing the polymers [10-12].

In this study, we have tried to use the well-known phase-inversion method, commonly employed for spinning polymeric hollow fiber membranes, to prepare the inorganic Al₂O₃ hollow fibers. Factors affecting the structure and performance of the membranes such as the spinning conditions, (change in air gap here) were studied extensively, and the formation procedure of the ceramic hollow fiber membrane was also discussed.

Experimental

1. Materials

AKP 30 α -Al₂O₃ (Al₂O₃, particle size of 0.3 μ m) from (Sumitomo Chemicals Co. LTD, Japan). Polyether sulfone (PES, Ultrason, 6020P, BASF, Germany) was used as polymer and N-methyl pyrrolidone (NMP, 99.5 wt%, Aldrich, The Netherlands) as solvent. PES, α -Al₂O₃ powder were dried before use.

2. Spinning process

Based on the principle of phase inversion of a particle loaded polymer solution the green fibers were prepared via dry-wet spinning process.

3. Drying and Thermal Treatment

After spinning the hollow fibers were kept directly in a water bath for 24 h for completion of the phase separation process (to remove the residual solvents), followed by drying for 24h to straighten the fiber. The fibers (15 cm length) were placed into the channels (4 mm) of a multichannel

Details of the spinning conditions are mentioned in Table 1.

Table 1: Spinning conditions

Condition	Value
Composition spinning mixture	see Table 2
Bore liquid	H ₂ O
External coagulant	H ₂ O
Mixture extrusion pressure (bar)	1
Air gap (cm)	0,2,15
Bore liquid flow rate (ml/min)	9
Spinneret diameter (mm)	OD/ID = 1.1/0.5
Temperature (°C)	21

Spinning mixture was prepared by adding the inorganic powder (see Table 2) to NMP, followed by stirring for 30 min. To decrease the amount of agglomerates, ultrasonic treatment was applied for the preparation of Al₂O₃ fibers for 30 min. PES was added in three steps, each separated by 2 h to prevent agglomerations, the mixture was then stirred for 16h to get a homogenous solution. The spinning mixture was degassed by applying vacuum for 30 min. Finally, the degassed spinning solution was pressurized by nitrogen. A tube-in-orifice spinneret (with inner diameter 0.5 mm and outer diameter 1.1 mm) was used to obtain hollow fiber precursors by wet spinning method at room temperature.

Table 2: Composition of spinning mixture of the performed experiment

Material	Concentration Particles in HF(vol%)	Particle size (μ m)	Spinning mixture			
			NMP (wt%)	PES (wt%)	Particle (wt%)	Viscosity (Pa/s)
Al ₂ O ₃	58	0.3	40	10	50	42

ceramic, subsequently placed horizontally in a furnace with a controlled atmosphere. A detailed program of the thermal treatment can be found in Table 3. A flow diagram showing the stages involved in the preparation of an inorganic hollow fiber is shown in Figure 1.

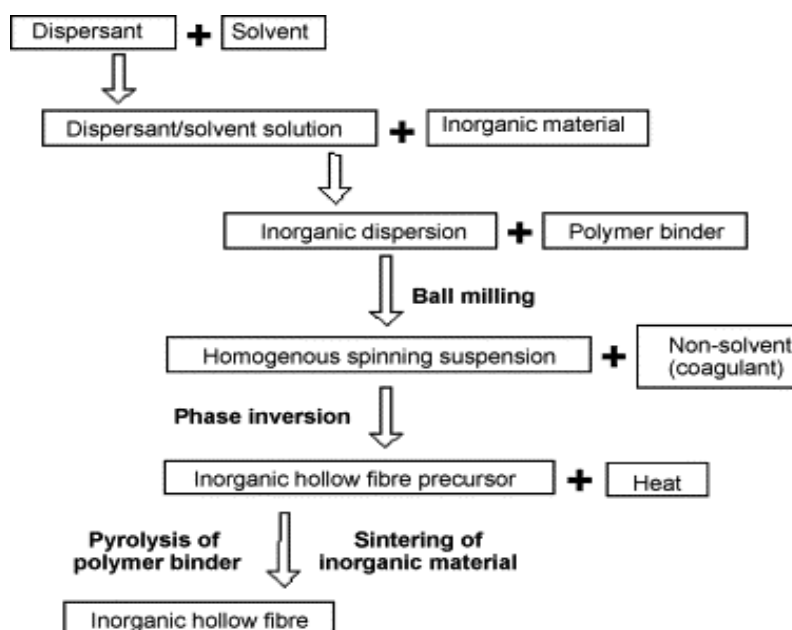


Fig. 1: Flow diagram showing the stages involved in the combined phase inversion and sintering technique for ceramic hollow fiber fabrication

Table 3: Sintering conditions

Temperature °C	Dwell Min	Rate °C/min
300	60	5
1400	120	5
25	-	5

4. Characterization

Viscosity data was collected (Physica UDS-200 rheometer) using cone and plate geometry at shear rates between 6 s^{-1} and 100 s^{-1} at $20 \text{ }^\circ\text{C}$. Spinning suspension samples were taken and tested immediately prior to fibre spinning. The prepared hollow fiber membranes structures were visually observed using a scanning electron microscope (JSM-6010LA). The inorganic hollow fiber membranes (after calcination), the clear cross sectional fracture could be obtained by directly snapping the fiber. These membrane samples were then positioned on a metal holder and gold-coated using sputter-coating operated under vacuum conditions. The SEM micrographs of both the surface and cross-section of the hollow fiber membranes were taken at various magnifications.

Results and Discussion

Figure 2 a–c shows precursor fibres spun with air gaps of 0 cm, 2 cm and 15 cm, an internal coagulant flow rate of 9 ml/min and an extrusion velocity of approximately 35 mm/s . It can be seen from Figure 2 a that the morphology of fibres spun directly into a non-solvent bath, i.e. a 0-cm air-gap consists of finger-like voids originating from both the inner and outer fibre surfaces which extend almost to the centre of the fibre cross-section. The morphology of the fibre shown in Figure 2 a is believed to result from hydrodynamically unstable viscous fingering occurring simultaneously and to a similar extent at both the inner and outer fibre surfaces, this result is in agreement with [13]. A central sponge-like region is present which provides the majority of the mechanical strength and separation characteristics. Maximum void length is approximately the same for voids originating from both the inner and outer surfaces and as in all the prepared fibres a void length distribution exists, some being only a few microns in length while others penetrate far into the fibre cross-

section. This structure may not be ideal for some of the principal applications of ceramic hollow fibre membranes such as solvent filtration which generally require the separation layer (packed pore mostly originated from the sponge-like region after heat treatment) to be at either the inner or outer edge. However, the above structure may be beneficial for the development of catalytic membranes, as finger-like voids may serve as substrates for catalyst particle impregnation. For example, a multifunctional catalytic membrane could be developed with different catalytic functions at the inner and outer surfaces with the central region of the membrane determining the permeation characteristics. This could be achieved by depositing two different types of catalyst targeted at different reactions within the inner and outer finger-like voids, respectively. Figure 2 b shows the fibre morphology resulting from a 2 cm air gap. As shown, the finger-like voids extend from the inner surface across approximately 50% of the fibre cross-section but void length at the outer surface has been greatly reduced. A sponge-like region occupying approximately 35% of the fibre cross-section is present between the inner and outer finger-like voids. The size and number of voids at the outer edge are further reduced when the air-gap is increased to 15 cm as shown in Figure 2 c. As can be seen, fingerlike voids extend from the inner surface across approximately 80% of the fibre cross-section with the remaining 20% consisting of a sponge-like region. Close examination of the outer edge of the fibre, as shown in Figure 2 d at increased magnification, reveals

Previous studies have shown that densification of sponge-like regions occurs during calcination, causing a decrease in porosity, eventually

resulting in a gas tight membrane at high calcination temperatures and high $\text{Al}_2\text{O}_3/\text{PES}$ ratios [6, 9, 14]. A comparison of Figure 2 c and f of precursor and calcined fibres spun with an air-gap of 15 cm suggests that similar results have also been observed in this work and that finger-like voids are retained during calcination despite the densification of the sponge-like structure. The situation is somewhat different when a 2 cm air gap is present. In this case simultaneous solvent evaporation and moisture (non-solvent) condensation causes a local viscosity increase in the outer region of the fibre prior to immersion. During the time the precursor fibre is exposed to the atmosphere (2 cm air gap), the viscosity of the outer region increases and finger-like voids originating at the inner surface penetrate into the fibre cross-section. As the precursor fibre makes contact with the non-solvent bath the increased viscosity of the outer region, as a result of exposure to the atmosphere, inhibits the growth of finger-like voids at the outer edge. However, non-solvent influx from the precipitation bath does still occur, further increasing the suspension viscosity as it penetrates the nascent fibre cross-section. This increases the viscosity in front of finger-like voids growing from the inner surface, limiting their length to approximately 50% of the fibre cross-section. Therefore finger-like voids forming from the inner surface can be increased in length by increasing the air-gap to 15 cm as shown in Figure 2 c. Under these conditions the viscosity of the outer region is higher when the nascent fibre is immersed and non-solvent influx is reduced, while at the same time voids originating at the inner surface have more time to penetrate further towards the outer edge.

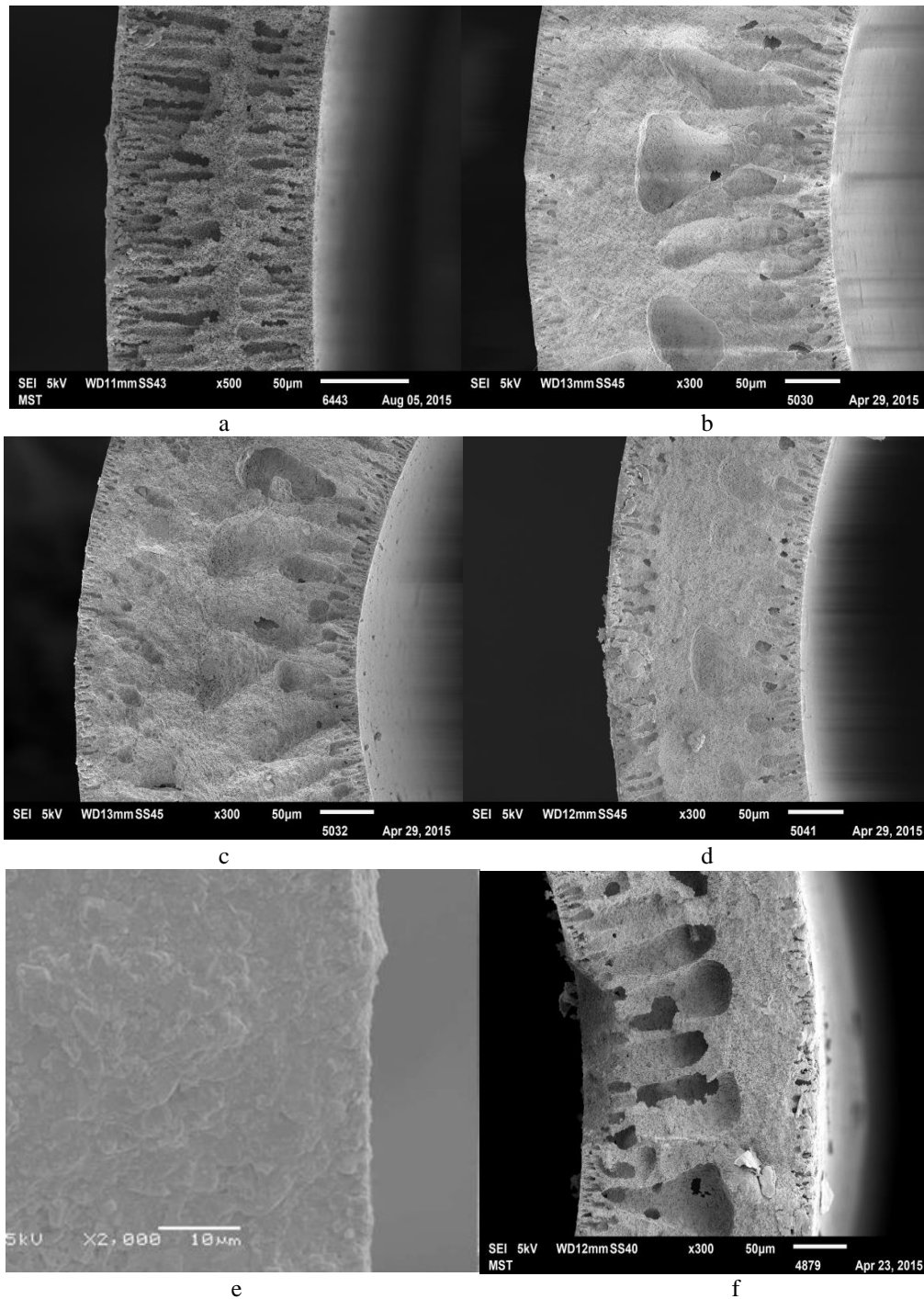


Fig. 2: Cross-sectional images of fibres 1-3—(a–c): precursor fibres, (d–f): sintered fibres; (a): fibre 1, 0 cm air-gap, (b): fibre 2, 2 cm air-gap, (c): fibre 3, 15 cm air-gap, (d) outer edge of fibre 3 (15 cm air-gap) calcined at 1400°C, (e) outer edge of fibre 3 (15 cm air-gap) calcined at 1600°C and (f): fibre 3, (15 cm air-gap) calcined at 1400°C

Conclusions

Finger-like voids in hollow fibres prepared from alumina/NMP/polyethersulfone spinning suspensions result from hydrodynamically unstable viscous fingering occurring at the interface

between the suspension and the non-solvent. Above a critical suspension viscosity this phenomenon is not observed and a sponge-like membrane structure is formed. By varying the viscosity of the spinning suspension by using water as a non-solvent

additive, fibre morphology can be varied greatly. Exposure of the outer fibre surface to the atmosphere causes a local viscosity increase and inhibits the formation of finger-like voids in this region. However, non-solvent may diffuse through this outer layer as the fibre is immersed, halting finger-like void growth from the inner surface and creating isolated voids within the membrane cross-section if the internal coagulant flow rate is insufficient. The air-gap and suspension viscosity are critical in determining both the formation of finger-like voids and the density of the outer sponge-like region. The addition of water as a non-solvent additive to the spinning suspension causes an increase in viscosity, a reduction in finger-like void length and favours the formation of a sponge-like structure at the outer fibre surface if an air-gap is present.

Acknowledgment

The author gratefully acknowledge the research funding provided by SHELL in IRAQ . A training program provided by MESA, University of Twente, Enschede, The Netherlands.

References

1. R.W. Baker, Membrane Technology and Applications, 2nd ed, McGraw-Hill, Chchester, (2004).
2. I. Moch, Hollow-fiber membranes, Kirk-Othmer encyclopedia of chemical technology ,in: Kirk-Othmer Encyclopedia of Chemical Technology, Willey, (2005).
3. M. Mulder, Basic Principles of Membrane Technology. 1st ed, Kluwer Academic Publishers, Dordrecht, (2000).
4. R.A. Terpstra, J.P.G.M. Van Eijk, F.K. Feenstra, Method for the production of ceramic hollow fibers, US Patent No. 5,707,584 (1998).
5. K.H. Lee, Y.M. Kim, Asymmetric hollow inorganic membranes, Key Eng. Mater. 61/62 ,17, (1991).
6. M.W.J. Luiten-Olieman, L. Winnubst, A. Nijmeijer, M. Wessling, N.E. Benes, Porous stainless steel hollow fiber membranes via dry-wet spinning, Journal of Membrane Science 370, 124–130, (2011).
7. B. Kingsbury, K. Li, A morphological study of ceramic hollow fibre membranes, Journal of Membrane Science 328, 134–140, (2009).
8. S.-M. Lee, I.-H. Choi, S.-W. Myung, J.-Y. Park, I.-C. Kim, W.-N. Kim, K.-H. Lee, Preparation and characterization of nickel hollow fiber membrane, DES 233, 32–39, (2008).
9. Patrick de Wit , Emiel J. Kappert , Theresa Lohaus, Matthias Wessling, Arian Nijmeijer, Nieck E. Benes, Highly permeable and mechanically robust silicon carbide hollow fiber membranes, Journal of Membrane Science 475, 480–487, (2015).
10. J.E. Koresh, A. Sofer, Molecular sieve carbon perm selective membrane. Part I. Presentation of a new device for gas mixture separation, Sep. Sci. Technol. 18, 723, (1983).
11. J.E. Koresh, A. Sofer, Mechanism of permeation through molecular-sieve carbon membrane, J. Chem. Soc., Faraday Trans. 82, 2057, (1986).
12. V.M. Linkov, R.D. Sanderson, E.P. Jacobs, Highly asymmetrical carbon membranes, in: Proceedings of the 34th IUPAC Symposium on Macromolecules, Vol. 7, p. 56 , (1992).
13. Benjamin F.K. Kingsbury, Zhentao Wu, K. Li, A

morphological study of ceramic hollow fibre membranes: A perspective on multifunctional catalytic membrane reactors, *Catalysis Today*, 156, 306-315, (2011).

14. S. Liu, K. Li, R. Hughes, Preparation of porous aluminium oxide (Al_2O_3) hollow fibre membranes by a combined phase-inversion and sintering method, *Ceram.Int.* 29, (8), 875–881, (2003).